Nuclear Inst. and Methods in Physics Research, A 959 (2020) 163543

Contents lists available at ScienceDirect

Nuclear Inst. and Methods in Physics Research, A

journal homepage: www.elsevier.com/locate/nima

Technical notes

Superconducting nanowires as high-rate photon detectors in strong magnetic fields

T. Polakovic [a,d], W.R. Armstrong [a], V. Yefremenko [b], J.E. Pearson [c], K. Hafidi [a], G. Karapetrov [d,e], Z.-E. Meziani [a], V. Novosad [c,*]

[a] Physics Division, Argonne National Laboratory, Argonne, IL, United States of America
[b] High Energy Physics Division, Argonne National Laboratory, Argonne, IL, United States of America
[c] Materials Science Division, Argonne National Laboratory, Argonne, IL, United States of America
[d] Department of Physics, Drexel University, Philadelphia, PA, United States of America
[e] Department of Materials Science and Engineering, Drexel University, Philadelphia, PA, United States of America

A B S T R A C T

Superconducting nanowire single photon detectors are capable of single-photon detection across a large spectral range with near unity detection efficiency, picosecond timing jitter, and sub-10 μm position resolution, at rates as high as 10^9 counts/s. In an effort to bring this technology into nuclear physics experiments, we fabricate niobium nitride (NbN) nanowire detectors using ion beam assisted sputtering and test their performance in strong magnetic fields. We demonstrate that these devices are capable of detection of 400 nm wavelength photons with saturated internal quantum efficiency at temperatures of 3 K and in magnetic fields of up to 5 T at high count rates and with nearly zero dark counts.

1. Introduction

Superconducting nanowire single photon detectors (SNSPD) are a relatively recent technology [1] but show great promise due to their detection capabilities that are in many aspects superior to more conventional semiconductor detectors: timing jitter (FWHM of the distribution of deviation from an ideal periodic single-photon response) shorter than 15 ps [2], near-unity detection efficiency [3], and count rates higher than 10^9 counts/s with 10^{-3} counts/s dark counts [4]. These metrics make SNSPDs a popular choice in fields of quantum communication and sensing, where they have been used in quantum key distribution [5], long-range quantum teleportation experiments [6,7], or LIDAR systems [8]. While SNSPDs are inherently a broadband detector and there are efforts to fabricate efficient devices for use in the UV and visible range [9,10], most of the mentioned applications work with standardized IR telecom wavelengths, so the detector development is focused on optimization of detection efficiency of low energy photons [3,11–14]. The situation is, however, different if one would want to use SNSPDs for experiments in nuclear physics, where potential applications would include detection of Cherenkov radiation, light from ionization or from a scintillator, and active polarized targets [15], where the spectral density is shifted toward visible–UV range [16], or as a part of detectors where it can be utilized for direct detection of α– and β–particles [17] or electrons [18]. Because SNSPDs have a trivial footprint, they can be positioned closer to the active area of the experiment and in this case we need to focus on performance in conditions that are typically not seen in experiments related to quantum communication. The complications associated with these environments are primarily large magnetic fields [19] and, often times, liquid helium temperatures [15], at which SNSPDs are known to outperform Si-based detectors [20]. As SNSPDs are superconducting detectors, cryogenic environments do not degrade their performance. On the other hand, their detection capabilities in strong magnetic fields have not been extensively studied, and so far, SNSPD characterization has usually been limited to fields smaller than 0.2 T [21–23].

In this work we explore photon detection capabilities at 400 nm wavelength in high magnetic fields and we show that, by using the recently developed ion beam assisted sputtering [24], we can fabricate niobium nitride (NbN) high-rate, low dark-count SNSPDs capable of operation at 3 K and in magnetic fields as high as 5 T. This fabrication process greatly reduces the complexity associated with producing SNSPDs designed for high-field operation [25] and provides dramatic performance increase compared to Si-based detectors [20,26] in similar environments.

2. Device fabrication

The detectors used in this work have the standard meander geometry, with a wire thickness of 13.5 nm, wire width of 80 nm, spacing between the wires of 110 nm and a pixel size of 10 × 10 μm^2 (as shown in Fig. 1b). The stoichiometric NbN thin films were prepared by ion beam assisted sputtering [24] at room temperature, with Ar as sputtering gas at 2 × 10^{-3} Torr in a ultra-high vacuum sputtering

* Corresponding author.
E-mail address: novosad@anl.gov (V. Novosad).

https://doi.org/10.1016/j.nima.2020.163543
Received 14 November 2019; Received in revised form 8 January 2020; Accepted 25 January 2020
Available online 31 January 2020
0168-9002/

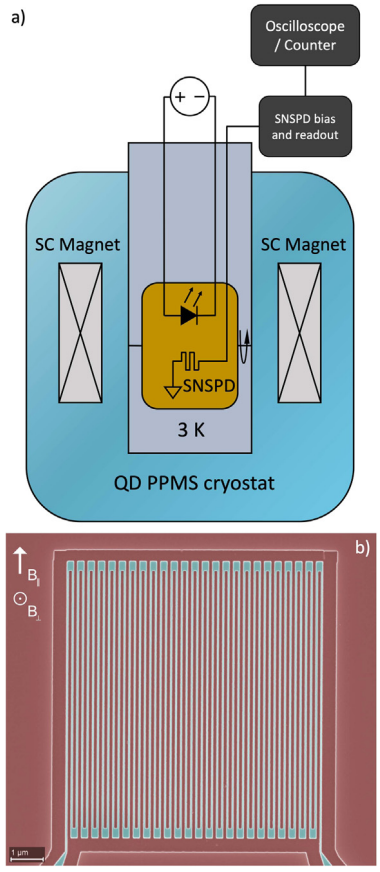

Fig. 1. Top: Scheme of the experimental setup used for measurement. The sample holder depicted in yellow rotates around the horizontal axis to change orientation of magnetic field relative to the SNSPD. Bottom: False color SEM micrograph of the fabricated nanowire detector, where the active current-carrying device is colored in teal. Field directions used in this experiment are depicted in the top-left corner. The voltage is sampled at the vicinity of the two points where the meander is connected to the external wiring. (For interpretation of the references to color in this figure legend, the reader is referred to the web version of this article.)

system from Angstrom engineering [27]. Devices were patterned using electron beam lithography and ZEP 520A diluted at 1:2 with anisol as resist. Nanowires were etched by reactive ion etching in CF_4 plasma.

Films before patterning had a superconducting critical temperature $T_C = 8$ K and normal sheet resistance of approximately 683 Ω. The perpendicular critical magnetic field was determined to be $H_{C2}(0) = 32$ T and the coherence length $\xi(0) = 3.2$ nm [24]. After patterning, the nanowire detector's T_C remained unchanged and the critical current density was determined to be $j_C(T = 3K) = 2.2 \times 10^{10}$ A/m^2 using voltage criterion of 2 µV across the total length of the meander (approximately 700 µm).

3. Experimental setup

A Quantum Design Physical Property Measurement System (PPMS) was used to control temperature and apply magnetic field during measurement. The characterization apparatus consisted of a custom designed PPMS insert manufactured by Quantum Opus LLC coupled with an Opus One SNSPD bias and readout module [28] and R&S RTM3000 oscilloscope (Fig. 1a). The signal was measured using a two-point voltage readout. Light to the detectors was supplied from flood illumination by InGaN LED integrated into the PPMS insert. Nominal wavelength of the LED was 465 nm at room temperature and, when cooled to operational temperature, the wavelength blueshifted to approximately 400 nm. Unless otherwise specified, the LED forward bias was set

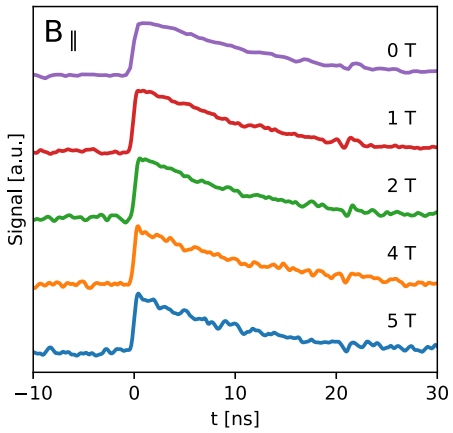

Fig. 2. Waterfall plot of typical single-photon voltage pulse waveforms at various in-plane magnetic fields. All signals are normalized to their respective pulse maximum and signal baseline can be seen at negative times.

to 30 µA to minimize excess device heating. All measurements of photoresponse and critical currents were conducted at temperatures of 3 K due to better temperature stability. We observe negligible change in performance at 4 K. All measurements in magnetic fields were carried out by zero-field cooling to 3 K before applying the magnetic field.

4. Results

In this work, we explore the device performance in two field configurations: one is in magnetic field applied parallel to the device plane ($B_\parallel$) and one with field perpendicular to the device plane ($B_\perp$) as schematically shown in Fig. 1b. Typical time trace of photon detection events can be seen in Fig. 2. The 20%–80% rise time was determined to be $\tau_R = 341 \pm 31$ ps and 80%–20% fall time is $\tau_F = 11.78 \pm 1.6$ ns. These values did not change significantly as a function of applied field or light intensity.

The other important detection characteristics, quantum efficiency and detection rate, of an SNSPD device can be extracted from the dependence of the count rate on device's bias current. At low currents, the probability of quasi-particle excitation and formation of a hot-spot region after photon absorption is low [29,30] and the probability increases with increasing bias current. As one increases the constant current bias of a device further, the count rate reaches a plateau — the saturated internal efficiency [31,32], where the probability of detecting an absorbed photon is close to unity [23,33]. At these current values, the total detection efficiency is determined by external parameters such as geometric filling factors [34] and optical coupling [35].

In the case of 400 nm photons in zero magnetic field, our devices can reach saturated internal efficiency at bias currents of approximately 9 µA, well below the critical currents of 23 µA (current density close to j = 2.2 × 10^{10} A/m^2). This means that the devices are capable of high detection rate with close to zero dark counts. The dark counts increase exponentially as the bias current reaches the critical value (Fig. 3). The average measured count rate with our devices was approximately 10^7 counts/s for the 100 µm^2 active area of the SNSPD detector with LED biased at 20 µA DC current. The detector count rate up to these values of the bias current is linear with the DC bias current of the LED (Fig. 4). Based on the LED parameters (120° apex angle, 56 mcd at 465 nm) and the distance between the LED and the detector (2 cm), the estimated photon flux on the detector area is on the order of 10^7 photons/s, corresponding to 100 ns between photon capture events (and linearly proportional to the LED forward bias current). The time between single photon absorption events is an order of magnitude longer than the fall time of a single count event in Fig. 2 which confirms that we operate in the single-photon regime [36]. This is not

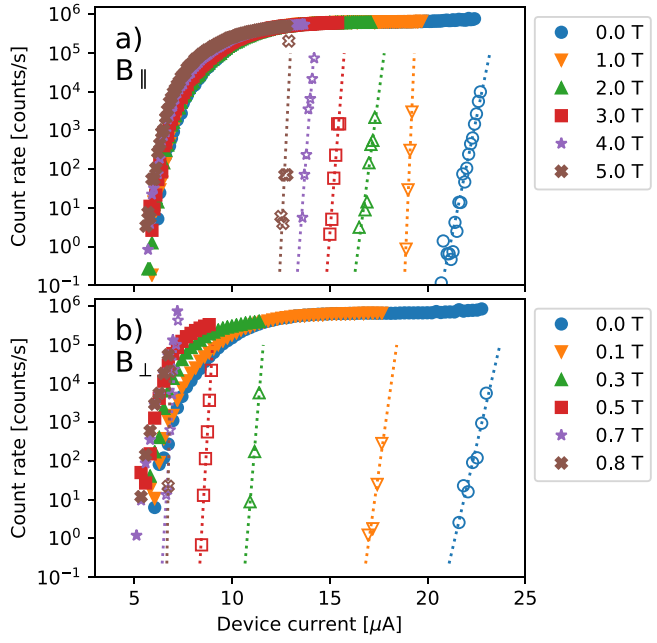

Fig. 3. Dependence of count rate as a function of nanowire bias current at various parallel magnetic fields at constant LED illumination intensity. Total counts are plotted with full circles, dark counts with empty circles. Dotted lines are exponential fits to the dark count rate data. Top and bottom figure corresponds to cases with parallel and perpendicular fields, respectively.

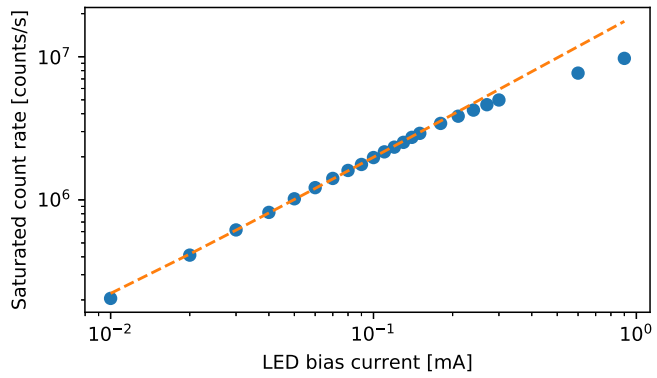

Fig. 4. Saturated count rate as a function of 400 nm LED forward bias current. In this small current forward bias regime, the light intensity is proportional to the InGaN LED current. Dashed line represents a linear fit the region up to 0.2 mA.

the maximum count rate capability of the SNSPD device (as can be seen from the trend in Fig. 4), but a limit imposed by the temperature control capabilities of our setup, at which the heat load of the LED exceeds the cooling power of the PPMS cryogenic setup. The deviation from the expected linear trend in Fig. 4 is attributed to these heating effects. In absence of this spurious heating, we expect our SNSPD devices to be capable of detection rates on the order of 10^8 counts/s — determined by the fall time, at which the count rate is close to $1/\tau_F$ [37]. If one desires to achieve higher count rates, common approaches include decreasing the length of the superconducting nanowire (to decrease the kinetic inductance of the device L_K [38]) or introducing a shunt resistance R_S to decrease the fall time constant $\tau_F \propto L_K/R_S$ or to split the wire into multiple segments connected in parallel so that the total inductance is a harmonic mean of the individual segment inductances [39,40].

Before we analyze the detector performance in applied magnetic fields, we briefly discuss the superconducting critical currents of the nanowires without LED illumination. The observed power law dependence of superconducting critical current I_C on magnetic field can be explained by the vortex dynamics in a type-II superconductor with strong edge pinning where the current should be inversely proportional to the applied field [41]:

$$j_C(B) = j_C(0) \cdot \frac{\mathcal{B}}{2B}, \tag{1}$$

where $\mathcal{B} = \frac{\Phi_0}{2\pi}\frac{1}{W\xi_{GL}}$ is the vortex penetration field, with Φ_0 being the Abrikosov flux quantum, W the wire width and ξ_{GL} the Ginzburg–Landau superconducting coherence length. However, our data does not fit a functional form proportional to $B^{-\alpha}$ with $\alpha \approx 1$, but rather $\alpha = 0.4$ in perpendicular magnetic fields (Fig. 5b) and $\alpha = 0.02$ in the case of fields parallel to the meander (Fig. 5a). The case of perpendicular fields, with $\alpha \approx 0.5$, has been observed in similar superconducting nanostructures before and can be explained by strong bulk vortex pinning [42] – as one would anticipate from materials with high density of lattice defects like our films grown by ion beam assisted sputtering. In the case of magnetic fields parallel to the transport current, the Lorenz force acting on the vortex lines is effectively zero (zero-force configuration). In this configuration the critical current density becomes a function of only the number of vortices in the wire [43] which greatly decreases the magnetic field dependence of the critical current [44], as can be seen in our measurements (Fig. 5a and, subsequently, Fig. 3a).

When analyzing magnetic field dependence of the detector response, we will first discuss the case of magnetic field applied perpendicular to the device plane (see Fig. 3b) which can be compared to the results in literature [21–23]. We see a relatively strong deterioration of detection capabilities even at fields below 1 T. This can be explained by the dynamics of the supercurrents [45] and superconducting vortices [46] in external magnetic field. Our choice of fabricating these devices out of NbN, deposited by ion beam assisted sputtering [24], has already led to a considerable improvement in capability of magnetic field performance when compared to similar devices studied in literature [21–23] (our devices can still detect photons in fields twice as large). This means, that with no additional engineering optimization we achieve results comparable to devices with geometry designed for performance in strong magnetic fields [25]. The practical limit of external perpendicular magnetic field is around 0.5 T, past which the detection is dominated by dark counts arising from fluctuations of the near-critical superconducting state [47,48]. One can increase this value by engineering a stronger thermal coupling to the heat sink (i.e. the substrate) [49], introducing stronger vortex pinning centers to minimize vortex creep and vortex hopping [50], optimizing the device geometry to prevent current crowding at the meander turns [25,51], or by increasing the wire cross-section. The increase in wire spacing or wire volume as in the last two approaches, however, leads to a decrease in total detection efficiency by sacrificing the geometric filling ratio (area of the pixel covered with superconductor divided by the total pixel area) or the hot-spot expansion probability, respectively.

As many experimental setups in nuclear physics are axially symmetric, with magnetic field applied along the symmetry axis (e.g. central solenoids in particle collider detectors [52,53]), it is also important to explore the behavior of the SNSPD devices in external fields aligned parallel to the detector plane. The quantitative dependence of count rate as a function of bias current in parallel magnetic fields is different, as can be seen in the results plotted in Fig. 3a. The detector reaches internal efficiency saturation in parallel magnetic fields as high as 5 T (the highest field achievable with our experimental setup), with device saturating at approximately 10 μA, well below the onset of dark counts at 12.5 μA. By extending the trend in Fig. 5c, we can make a conservative estimate of the limiting parallel magnetic field to be approximately 8 T, assuming that the saturation current is independent of the applied magnetic field. The assumption of constant saturation current does not necessarily hold, as seen in Fig. 3, where the onset of saturation happens at lower bias currents. This behavior is assumed

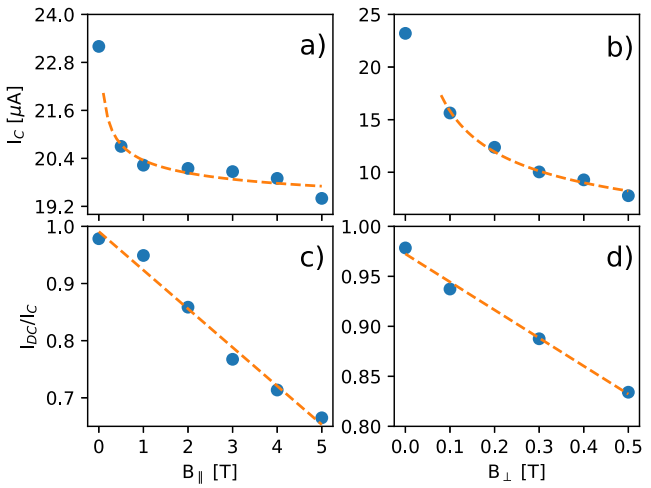

Fig. 5. Dependence of superconducting critical currents I_C (top row) and the normalized detector critical currents I_{DC}/I_C (bottom row) on applied magnetic fields. Left and right column corresponds to parallel and perpendicular field orientations, respectively. Dashed lines in are fits of linear dependence in plots (c) and (d), and $B^{-\alpha}$ dependence in (a) and (b).

to be due to effects of superconducting vortices, which can assist the hotspot formation and expansion [46]. It is important to mention that the magnetic field effects on the saturation current are relatively weak and lead to underestimation of the limiting magnetic field, so we believe that the value of 8 T is still a reasonable approximation, even if we are unable to reach magnetic fields of such magnitudes in our setup.

As the physics driving the parallel field dependence is similar to the situation in perpendicular magnetic fields, one can use similar approaches to increase the value of critical magnetic fields: increasing the wire thickness and thermal coupling, changing material microstructure to introduce additional vortex pinning sites, and optimizing the meander turn geometry to decrease the current densities near the turns.

5. Conclusion

We have demonstrated that superconducting nanowire single photon detectors are a viable technology for detection of individual photons in strong magnetic fields. We show that detectors fabricated from NbN grown by ion beam assisted sputtering can withstand strong magnetic fields as high as 5 T in configurations with magnetic field parallel to the pixel plane and 0.5 T in perpendicular configurations, which is double the commonly reported field strength reported in the literature. Even at such large fields SNSPDs are capable of high-rate detection of 400 nm photons (potentially up to 10^8 count/s at 100 μm^2 pixel size) with less than 1 dark counts per second, which makes them an attractive alternative for high-rate, high-background measurements in strong field environments — a common demand in nuclear physics experiments that cannot be met by conventional semiconductor detectors in the similar environments.

Declaration of competing interest

The authors declare that they have no known competing financial interests or personal relationships that could have appeared to influence the work reported in this paper.

CRediT authorship contribution statement

T. Polakovic: Conceptualization, Methodology, Investigation, Visualization, Formal analysis, Writing - original draft. **W.R. Armstrong:** Conceptualization, Methodology, Writing - review & editing. **V. Yefremenko:** Methodology, Investigation, Writing - review & editing. **J.E. Pearson:** Methodology, Investigation, Writing - review & editing. **K. Hafidi:** Project administration, Writing - review & editing. **G. Karapetrov:** Conceptualization, Methodology, Supervision, Writing - review & editing. **Z.-E. Meziani:** Conceptualization, Methodology, Project administration, Writing - review & editing. **V. Novosad:** Conceptualization, Methodology, Data curation, Supervision, Writing - review & editing.

Acknowledgments

We would like to thank Dr. Aaron Miller from Quantum Opus LLC for fruitful discussions and assistance in detector characterization setup and Dr. Ralu Divan from Argonne National Laboratory's Center for Nanoscale Materials for help with the development of nanofabrication protocols.

This work was supported by the U.S. Department of Energy (DOE), Office of Science, Office of Nuclear Physics and Office of Basic Energy Sciences, Materials Sciences and Engineering Division (thin film materials synthesis and characterization) under Contract No. DE-AC02-06CH11357. The work was performed, in part, at the Center for Nanoscale Materials, a U.S. Department of Energy Office of Science User Facility, and supported by the U.S. Department of Energy, Office of Science, Office of Basic Energy Sciences, under Contract No. DE-AC02-06CH11357.

References

[1] G. Gol'Tsman, O. Okunev, G. Chulkova, A. Lipatov, A. Semenov, K. Smirnov, B. Voronov, A. Dzardanov, C. Williams, R. Sobolewski, Picosecond superconducting single-photon optical detector, Appl. Phys. Lett. 79 (6) (2001) 705–707.

[2] J. Wu, L. You, S. Chen, H. Li, Y. He, C. Lv, Z. Wang, X. Xie, Improving the timing jitter of a superconducting nanowire single-photon detection system, Appl. Opt. 56 (8) (2017) 2195–2200.

[3] F. Marsili, V.B. Verma, J.A. Stern, S. Harrington, A.E. Lita, T. Gerrits, I. Vayshenker, B. Baek, M.D. Shaw, R.P. Mirin, et al., Detecting single infrared photons with 93% system efficiency, Nature Photon. 7 (3) (2013) 210.

[4] H. Shibata, K. Shimizu, H. Takesue, Y. Tokura, Ultimate low system dark-count rate for superconducting nanowire single-photon detector, Opt. Lett. 40 (14) (2015) 3428–3431.

[5] H. Takesue, S.W. Nam, Q. Zhang, R.H. Hadfield, T. Honjo, K. Tamaki, Y. Yamamoto, Quantum key distribution over a 40-db channel loss using superconducting single-photon detectors, Nature Photon. 1 (6) (2007) 343.

[6] H. Takesue, S.D. Dyer, M.J. Stevens, V. Verma, R.P. Mirin, S.W. Nam, Quantum teleportation over 100 km of fiber using highly efficient superconducting nanowire single-photon detectors, Optica 2 (10) (2015) 832–835.

[7] R. Valivarthi, Q. Zhou, G.H. Aguilar, V.B. Verma, F. Marsili, M.D. Shaw, S.W. Nam, D. Oblak, W. Tittel, et al., Quantum teleportation across a metropolitan fibre network, Nature Photon. 10 (10) (2016) 676.

[8] J. Zhu, Y. Chen, L. Zhang, X. Jia, Z. Feng, G. Wu, X. Yan, J. Zhai, Y. Wu, Q. Chen, et al., Demonstration of measuring sea fog with an snspd-based lidar system, Sci. Rep. 7 (1) (2017) 15113.

[9] E.E. Wollman, V.B. Verma, A.D. Beyer, R.M. Briggs, B. Korzh, J.P. Allmaras, F. Marsili, A. Lita, R. Mirin, S. Nam, et al., Uv superconducting nanowire single-photon detectors with high efficiency, low noise, and 4 k operating temperature, Opt. Express 25 (22) (2017) 26792–26801.

[10] D.H. Slichter, V.B. Verma, D. Leibfried, R.P. Mirin, S.W. Nam, D.J. Wineland, Uv-sensitive superconducting nanowire single photon detectors for integration in an ion trap, Opt. Express 25 (8) (2017) 8705–8720.

[11] F. Bellei, A.P. Cartwright, A.N. McCaughan, A.E. Dane, F. Najafi, Q. Zhao, K.K. Berggren, Free-space-coupled superconducting nanowire single-photon detectors for infrared optical communications, Opt. Express 24 (4) (2016) 3248–3257.

[12] F. Marsili, V. Verma, M. Stevens, J. Stern, M. Shaw, A. Miller, D. Schwarzer, A. Wodtke, R. Mirin, S. Nam, Mid-infrared single-photon detection with tungsten silicide superconducting nanowires, in: CLEO: Science and Innovations, Optical Society of America, 2013, pp. CTu1H–1.

[13] M. Csete, Á. Sipos, F. Najafi, X. Hu, K.K. Berggren, Numerical method to optimize the polar-azimuthal orientation of infrared superconducting-nanowire single-photon detectors, Appl. Opt. 50 (31) (2011) 5949–5956.

[14] Y. Wang, H. Li, L. You, C. Lv, J. Huang, W. Zhang, L. Zhang, X. Liu, Z. Wang, X. Xie, Broadband near-infrared superconducting nanowire single-photon detector with efficiency over 50%, IEEE Trans. Appl. Supercond. 27 (4) (2016) 1–4.

[15] M. Biroth, A. Thomas, P. Achenbach, E. Downie, Design of the mainz active polarized target, PoS (2016) 005.

[16] M. Nikl, A. Yoshikawa, K. Kamada, K. Nejezchleb, C. Stanek, J. Mares, K. Blazek, Development of luag-based scintillator crystals–a review, Progr. Crystal Growth Character. Mater. 59 (2) (2013) 47–72.
[17] H. Azzouz, S.N. Dorenbos, D. De Vries, E.B. Ureña, V. Zwiller, Efficient single particle detection with a superconducting nanowire, AIP Adv. 2 (3) (2012) 032124.
[18] M. Rosticher, F. Ladan, J. Maneval, S. Dorenbos, T. Zijlstra, T. Klapwijk, V. Zwiller, A. Lupaşcu, G. Nogues, A high efficiency superconducting nanowire single electron detector, Appl. Phys. Lett. 97 (18) (2010) 183106.
[19] W.R. Armstrong, S. Choi, E. Kaczanowicz, A. Lukhanin, Z.-E. Meziani, B. Sawatzky, A threshold gas cherenkov detector for the spin asymmetries of the nucleon experiment, Nucl. Instrum. Methods Phys. Res. A 804 (2015) 118–126.
[20] M. Biroth, P. Achenbach, E. Downie, A. Thomas, Silicon photomultiplier properties at cryogenic temperatures, Nucl. Instrum. Methods Phys. Res. A 787 (2015) 68–71.
[21] A.A. Korneev, Y.P. Korneeva, M.Y. Mikhailov, Y.P. Pershin, A.V. Semenov, D.Y. Vodolazov, A.V. Divochiy, Y.B. Vakhtomin, K.V. Smirnov, A.G. Sivakov, et al., Characterization of mosi superconducting single-photon detectors in the magnetic field, IEEE Trans. Appl. Supercond. 25 (3) (2014) 1–4.
[22] A. Engel, A. Schilling, K. Il'in, M. Siegel, Dependence of count rate on magnetic field in superconducting thin-film tan single-photon detectors, Phys. Rev. B 86 (14) (2012) 140506.
[23] R. Lusche, A. Semenov, K. Il'in, Y. Korneeva, A. Trifonov, A. Korneev, H.-W. Hübers, M. Siegel, G. Gol'tsman, Effect of the wire width and magnetic field on the intrinsic detection efficiency of superconducting nanowire single-photon detectors, IEEE Trans. Appl. Supercond. 23 (3) (2012) 2200205.
[24] T. Polakovic, S. Lendinez, J.E. Pearson, A. Hoffmann, V. Yefremenko, C.L. Chang, W. Armstrong, K. Hafidi, G. Karapetrov, V. Novosad, Room temperature deposition of superconducting niobium nitride films by ion beam assisted sputtering, APL Mater. 6 (7) (2018) 076107.
[25] I. Charaev, A. Semenov, R. Lusche, K. Ilin, H.-W. Huebers, M. Siegel, Enhancement of critical currents and photon count rates by magnetic field in spiral superconducting nanowire single-photon detectors, IEEE Trans. Appl. Supercond. 26 (3) (2016) 1–4.
[26] J. Xie, M. Hattawy, M. Chiu, K. Hafidi, E. May, J. Repond, R. Wagner, L. Xia, Rate capability and magnetic field tolerance measurements of fast timing microchannel plate photodetectors, Nucl. Instrum. Methods Phys. Res. A 912 (2018) 85–89.
[27] https://angstromengineering.com/products/evovac/.
[28] https://www.quantumopus.com/web/product-info/.
[29] C.M. Natarajan, M.G. Tanner, R.H. Hadfield, Superconducting nanowire single-photon detectors: physics and applications, Supercond. Sci. Technol. 25 (6) (2012) 063001.
[30] F. Marsili, M.J. Stevens, A. Kozorezov, V.B. Verma, C. Lambert, J.A. Stern, R.D. Horansky, S. Dyer, S. Duff, D.P. Pappas, et al., Hotspot relaxation dynamics in a current-carrying superconductor, Phys. Rev. B 93 (9) (2016) 094518.
[31] B. Baek, A.E. Lita, V. Verma, S.W. Nam, Superconducting aw x si 1- x nanowire single-photon detector with saturated internal quantum efficiency from visible to 1850 nm, Appl. Phys. Lett. 98 (25) (2011) 251105.
[32] F. Najafi, A. Dane, F. Bellei, Q. Zhao, K.A. Sunter, A.N. McCaughan, K.K. Berggren, Fabrication process yielding saturated nanowire single-photon detectors with 24-ps jitter, IEEE J. Sel. Top. Quantum Electron. 21 (2) (2014) 1–7.
[33] F. Marsili, F. Najafi, E. Dauler, F. Bellei, X. Hu, M. Csete, R.J. Molnar, K.K. Berggren, Single-photon detectors based on ultranarrow superconducting nanowires, Nano Lett. 11 (5) (2011) 2048–2053.
[34] J.K. Yang, A.J. Kerman, E.A. Dauler, B. Cord, V. Anant, R.J. Molnar, K.K. Berggren, Suppressed critical current in superconducting nanowire single-photon detectors with high fill-factors, IEEE Trans. Appl. Supercond. 19 (3) (2009) 318–322.
[35] X. Hu, C.W. Holzwarth, D. Masciarelli, E.A. Dauler, K.K. Berggren, Efficiently coupling light to superconducting nanowire single-photon detectors, IEEE Trans. Appl. Supercond. 19 (3) (2009) 336–340.
[36] F. Najafi, J. Mower, N.C. Harris, F. Bellei, A. Dane, C. Lee, X. Hu, P. Kharel, F. Marsili, S. Assefa, et al., On-chip detection of non-classical light by scalable integration of single-photon detectors, Nature Commun. 6 (2015) 5873.
[37] A.J. Kerman, D. Rosenberg, R.J. Molnar, E.A. Dauler, Readout of superconducting nanowire single-photon detectors at high count rates, J. Appl. Phys. 113 (14) (2013) 144511.
[38] A.J. Kerman, E.A. Dauler, W.E. Keicher, J.K. Yang, K.K. Berggren, G. Gol'Tsman, B. Voronov, Kinetic-inductance-limited reset time of superconducting nanowire photon counters, Appl. Phys. Lett. 88 (11) (2006) 111116.
[39] M. Ejrnaes, A. Casaburi, O. Quaranta, S. Marchetti, A. Gaggero, F. Mattioli, R. Leoni, S. Pagano, R. Cristiano, Characterization of parallel superconducting nanowire single photon detectors, Supercond. Sci. Technol. 22 (5) (2009) 055006.
[40] R.M. Heath, M.G. Tanner, A. Casaburi, M.G. Webster, L. San Emeterio Alvarez, W. Jiang, Z.H. Barber, R.J. Warburton, R.H. Hadfield, Nano-optical observation of cascade switching in a parallel superconducting nanowire single photon detector, Appl. Phys. Lett. 104 (6) (2014) 063503.
[41] G. Maksimova, Mixed state and critical current in narrow semiconducting films, Phys. Solid State 40 (10) (1998) 1607–1610.
[42] Y.N. Ovchinnikov, B. Ivlev, Pinning in layered inhomogeneous superconductors, Phys. Rev. B 43 (10) (1991) 8024.
[43] G. Stejic, A. Gurevich, E. Kadyrov, D. Christen, R. Joynt, D. Larbalestier, Effect of geometry on the critical currents of thin films, Phys. Rev. B 49 (2) (1994) 1274.
[44] G. Carneiro, Equilibrium vortex-line configurations and critical currents in thin films under a parallel field, Phys. Rev. B 57 (10) (1998) 6077.
[45] H. Hortensius, E. Driessen, T. Klapwijk, K. Berggren, J. Clem, Critical-current reduction in thin superconducting wires due to current crowding, Appl. Phys. Lett. 100 (18) (2012) 182602.
[46] L.N. Bulaevskii, M.J. Graf, V.G. Kogan, Vortex-assisted photon counts and their magnetic field dependence in single-photon superconducting detectors, Phys. Rev. B 85 (1) (2012) 014505.
[47] T. Yamashita, S. Miki, K. Makise, W. Qiu, H. Terai, M. Fujiwara, M. Sasaki, Z. Wang, Origin of intrinsic dark count in superconducting nanowire single-photon detectors, Appl. Phys. Lett. 99 (16) (2011) 161105.
[48] A. Murphy, A. Semenov, A. Korneev, Y. Korneeva, G. Gol'tsman, A. Bezryadin, Three temperature regimes in superconducting photon detectors: quantum, thermal and multiple phase-slips as generators of dark counts, Sci. Rep. 5 (2015) 10174.
[49] M. Hofherr, D. Rall, K. Il'in, A. Semenov, H.-W. Hübers, M. Siegel, Dark count suppression in superconducting nanowire single photon detectors, J. Low Temp. Phys. 167 (5–6) (2012) 822–826.
[50] A. Larkin, Y.N. Ovchinnikov, Pinning in type ii superconductors, J. Low Temp. Phys. 34 (3–4) (1979) 409–428.
[51] M.K. Akhlaghi, H. Atikian, A. Eftekharian, M. Loncar, A.H. Majedi, Reduced dark counts in optimized geometries for superconducting nanowire single photon detectors, Opt. Express 20 (21) (2012) 23610–23616.
[52] A. Hervé, The cms detector magnet, IEEE Trans. Appl. Supercond. 10 (1) (2000) 389–394.
[53] J. Lighthall, B. Back, S. Baker, S. Freeman, H. Lee, B. Kay, S. Marley, K. Rehm, J. Rohrer, J. Schiffer, et al., Commissioning of the helios spectrometer, Nucl. Instrum. Methods Phys. Res. A 622 (1) (2010) 97–106.